Conglomeratic Solid Solutions in *trans*(*N*,*t*-*N*)-[Co(leucinato)(tren)]I_2 and *trans*(*N*,*t*-*N*)-[Co(norleucinato or norvalinato)(tren)][ClO_4]$_2$ [*t*-*N*=tertiary amine nitrogen; tren=tris(2-aminoethyl)amine]

Kazuaki Yamanari* and Akira Fuyuhiro

Department of Chemistry, Faculty of Science, Osaka University, Toyonaka, Osaka 560

(Received December 20, 1995)

Ternary solubility isotherms of *trans*(*N*, *t*-*N*)-[Co(leu)(tren)]I_2, *trans*(*N*, *t*-*N*)-[Co(n-leu)(tren)][ClO_4]$_2$, and *trans*(*N*, *t*-*N*)-[Co(n-val)(tren)][ClO_4]$_2$ [*t*-*N* = tertiary amine nitrogen; leu = leucinate(1-), n-leu = norleucinate(1-), n-val = norvalinate(1-), and tren = tris(2-aminoethyl)amine] were determined at 25 °C. Each isotherm consists of two branches of the solubility curve and one eutectic point; the tie lines do not converge to any apex of the pure enantiomers, but diverge widely. These facts mean that the three complexes simultaneously form a conglomerate and a solid solution. X-Ray crystal analyses were carried out for crystals grown from the three racemic aqueous solutions. All of the crystals were isomorphous to each other in spite of having different amino acidates and counter ions. The crystal structures clearly demonstrated the coexistence of D-amino acidate and L-amino acidate at one site of the crystal lattice, that is, a solid solution. Furthermore, all of the crystals were partially optically active: D : L = 63 : 37 for leu complex (space group $P3_2$), D : L = 32 : 68 for n-leu one ($P3_1$), and D : L = 44 : 56% for n-val one ($P3_1$). Head-to-tail hydrogen bonding contacts, which form spiral chains along the *c*-axis, were commonly found for these complexes.

Crystalline racemates belong to one of three different classes: a racemic compound, a conglomerate (racemic mixture), and a solid solution.[1] The latter two cases have so far been very limited. Recently, we have reported on the first examples of racemic solid solutions containing amino acidate in [Co(leu)(NH_3)$_4$]Br_2·H_2O and [Co(leu)(NH_3)$_4$]-I_2·H_2O [leu=leucinate(1-)].[2] The isotherms are flat and close to an ideal solid solution, because the solubilities of the racemate and the enantiomer are almost equal. An X-ray crystal structure analysis has shown that both complexes are isomorphous, and that all sites of the unit cell comprise almost equal amounts of the D- and the L-amino acidato complex ions in the racemic complex.

Another kind of solid solution has been reported in *trans*(*N*, *t*-*N*)-[Co(n-leu)(tren)]I_2 and *trans*(*N*, *t*-*N*)-[Co(met)(tren)]I_2 [*t*-*N* = tertiary amine nitrogen; n-leu = norleucinate(1-), met = methioninate(1-), tren = tris(2-aminoethyl)amine].[3] The ternary isotherms are slightly different from those of [Co(leu)(NH_3)$_4$]X_2 (X = Br and I).[2] The isotherms swell in the center part, because the racemate is less soluble than the enantiomer in both systems. Crystal analyses have revealed the co-existence of the D- and L-amino acidato complex ions at each site of the unit cell in both complexes; furthermore, the unit cell comprises two D-rich sites and two L-rich sites. An unequal occupancy of the D- and L-amino acidato complex ions at each site is found irrespective of the racemic composition.

These findings prompted us to carry out further investigations of the solubility phase diagrams as well as X-ray crystal analyses of other amino acidato complexes. In this paper we describe the preparations of the racemates and enantiomers in three systems: *trans*(*N*, *t*-*N*)-[Co(leu)(tren)]-I_2, *trans*(*N*, *t*-*N*)-[Co(n-leu)(tren)][ClO_4]$_2$, and *trans*(*N*, *t*-*N*)-[Co(n-val)(tren)][ClO_4]$_2$ [n-val = norvalinate(1-)]. The binary and ternary solubility isotherms for these systems were determined, which reveal the existence of unprecedented new solid solutions having both properties of a conglomerate and a solid solution. The results have definitely been confirmed by the X-ray crystal structures. The preliminary results are partially reported elsewhere.[4]

Experimental

Preparations of *trans*(*N*, *t*-*N*)-[Co(DL-leu)(tren)]I_2 (1), *trans*(*N*, *t*-N)-[Co(L-leu)(tren)]I_2 (2), *trans*(*N*, *t*-*N*)-[Co(DL-n-leu)(tren)][ClO_4]$_2$ (3), *trans*(*N*, *t*-*N*)-[Co(L-n-leu)(tren)][ClO_4]$_2$ (4), *trans*(*N*, *t*-*N*)-[Co(DL-n-val)(tren)][ClO_4]$_2$ (5), and *trans*(*N*, *t*-*N*)-[Co(D-n-val)(tren)][ClO_4]$_2$ (6). These complexes were prepared from [$Co(Cl)_2$(tren)]Cl, an equimolar amount of DL- or L-amino acid and KOH according to a method by Akamatsu et al.[5] In the case of n-val, D-amino acid was used as an optically active ligand. The desired iodide or perchlorate was obtained by adding a calculated amount of KI or $NaClO_4$ to the resultant chloride solution. In the DL-n-leu system, the double salt [Co(DL-n-leu)(tren)]I[ClO_4]·3.5H_2O was obtained instead of the perchlorate. The salt was converted to pure perchlorate using a column of QAE-Sephadex A-25 (ClO_4^- form). All of the complexes were recrystallized from water. In each system only the orange isomer was obtained, though two geometrical isomers are possible. The orange isomer was assigned to *trans*(*N*, *t*-*N*),[2,3] where the NH_2 group of amino acidate is positioned trans to the tertiary amine of tren. The yields were ca. 70—80%.

Complex **1** {Found: C, 24.51; H, 5.12; N, 11.84%. Calcd for *trans*(*N*,*t*-*N*)-[Co(DL-leu)(tren)]I_2 = $C_{12}H_{30}CoI_2N_5O_2$: C, 24.46; H, 5.13; N, 11.89%}: VIS (water) λ_{max}/nm 471 (ε/dm^3 mol^{-1} cm^{-1} 122.7) and 342 (116).

Complex **2** {Found: C, 24.34; H, 5.10; N, 11.81%. Calcd for *trans*(*N*,*t*-*N*)-[Co(L-leu)(tren)]I_2 = $C_{12}H_{30}CoI_2N_5O_2$: C, 24.46; H, 5.13; N, 11.89%}: VIS (water) λ_{max}/nm 471 (ε/dm^3 mol^{-1} cm^{-1} 122.7) and 342 (119): CD (water) λ_{ext}/nm 511 ($\Delta\varepsilon$/dm^3 mol^{-1} cm^{-1} +0.151), 455 (−0.760), and 343 (+0.127).

Complex **3** {Found: C, 27.21; H, 5.75; N, 13.10%. Calcd for *trans*(*N*,*t*-*N*)-[Co(DL-n-leu)(tren)][ClO_4]$_2$=$C_{12}H_{30}Cl_2CoN_5O_{10}$: C, 26.98; H, 5.66; N, 13.11%}: VIS (water) λ_{max}/nm 471 (ε/dm^3 mol^{-1} cm^{-1} 124.7) and 342 (112).

Complex **4** {Found: C, 26.87; H, 5.73; N, 13.04%. Calcd for *trans*(*N*,*t*-*N*)-[Co(L-n-leu)(tren)][ClO_4]$_2$ = $C_{12}H_{30}Cl_2CoN_5O_{10}$: C, 26.98; H, 5.66; N, 13.11%}: VIS (water) λ_{max}/nm 471 (ε/dm^3 mol^{-1} cm^{-1} 123.4) and 342 (110): CD (water) λ_{ext}/nm 510 ($\Delta\varepsilon$/dm^3 mol^{-1} cm^{-1} +0.188), 455 (−0.827), and 343 (+0.140).

Complex **5** {Found: C, 25.47; H, 5.53; N, 13.45%. Calcd for *trans*(*N*,*t*-*N*)-[Co(DL-n-val)(tren)][ClO_4]$_2$=$C_{11}H_{28}Cl_2CoN_5O_{10}$: C, 25.40; H, 5.43; N, 13.46%}: VIS (water) λ_{max}/nm 471 (ε/dm^3 mol^{-1} cm^{-1} 123.3) and 342 (116).

Complex **6** {Found: C, 25.49; H, 5.48; N, 13.43%. Calcd for *trans*(*N*,*t*-*N*)-[Co(D-n-val)(tren)][ClO_4]$_2$ = $C_{11}H_{28}Cl_2CoN_5O_{10}$: C, 25.40; H, 5.43; N, 13.46%}: VIS (water) λ_{max}/nm 471 (ε/dm^3 mol^{-1} cm^{-1} 125.6) and 342 (118): CD (water) λ_{ext}/nm 510 ($\Delta\varepsilon$/dm^3 mol^{-1} cm^{-1} −0.184), 455 (+0.810), and 343 (−0.143).

Solubility Measurements. The solubilities of complexes in water were determined according to the same procedure as previously reported.[2] The binary solubilities are collected in Table 1. In the ternary isotherm, the measurement of one point required stirring for ca. 24 h, because the establishment of a true solubility equilibrium would require a continuous change in the composition of the solid phase concomitantly with that of the solution. The composition of the equilibrated solution was determined on the basis of absorption (VIS) and circular dichroism (CD) spectral measurements. The composition of the solid in equilibrium with the solution was determined in the same way as described above using a solid sample free from the mother liquor. The solid compositions in equilibrium with the racemic solution, which correspond to point **P** or **Q** in Figs. 2, 3, and 4 (as shown below), were determined as follows. Some crystals were grown from the racemic solution at 25 °C; the compositions of the individual crystals were then determined by the VIS and CD spectra. The mean values of the 10—15 crystals correspond to the compositions at points **P** and **Q**. The solid phases were also identified by an elemental analysis and the infrared (IR) spectra. The ternary solubility data are collected in Table 2.

Table 1. Solubility of *trans*(*N*,*t*-*N*)-[Co(DL- or L-amino acidato)(tren)]X_2 (grams of anhydrous salt in 100 g of water)

	leu (X=I)			n-leu (X=ClO_4)		
T/°C	S_{DL}	S_L	S_{DL}/S_L	S_{DL}	S_L	S_{DL}/S_L
5.0	1.54	1.24	1.24	1.36	1.14	1.19
10.0	1.75	1.42	1.23	1.58	1.32	1.20
15.0	2.00	1.60	1.25	1.79	1.47	1.22
20.0	2.28	1.83	1.25	2.18	1.70	1.28
25.0	2.59	2.07	1.25	2.53	2.00	1.27
30.0	2.97	2.37	1.25	2.94	2.30	1.28
35.0	3.35	2.71	1.24	3.46	2.63	1.32
40.0	3.85[a)]	3.06[a)]	1.26	3.97	3.04	1.31
45.0	4.35	3.47	1.25	4.60	3.53	1.30
50.0	4.88	3.91	1.25	5.34	4.02	1.33
55.0	5.57	4.45	1.25			

a) Solubility value at 0.1 °C higher than the indicated temperature.

X-Ray Crystallography. Single crystals of the *trans*(*N*,*t*-*N*)-[Co(leu)(tren)]I_2 (**1′**), *trans*(*N*,*t*-*N*)-[Co(n-leu)(tren)][ClO_4]$_2$ (**3′**), and *trans*(*N*,*t*-*N*)-[Co(n-val)(tren)][ClO_4]$_2$ (**5′**) complexes were grown from their racemic aqueous solutions at 25 °C, and were mounted on glass fibers with epoxy cement. The data were collected on a Rigaku AFC5R diffractometer using graphite monochromated Mo $K\alpha$ radiation (λ =0.71069 Å) and solved by TEXSAN.[6] Block diagonal-matrix least-squares refinements were used. Both decay and absorption corrections were applied, and any redundant data were removed. The crystal data are given in Table 3.

Disordered parts appeared in all of the structures. They were asymmetric carbons (C(8)) and the side chains of amino acidates. The locations of amino acidato moieties were determined in the same way as described elsewhere.[4] For complexes **1′** and **3′**, the asymmetric carbons and the next carbons of the amino acidates were separated to A and B sites; for complex **5′**, however, only the asymmetric carbon could be separated. The terminal atoms of the side chains were solved as an accidental overlap for simplicity. The occupancies of the minimum R values were A : B = 63 : 37, 68 : 32, and 56 : 44(%) for complexes **1′**, **3′**, and **5′**, respectively. These ratios agree well with the results of the solubility measurements. All non-hydrogen atoms were refined anisotropically, and the hydrogens of tren were located at the calculated positions; all other hydrogens were neglected.

The absolute configurations were determined at almost the final stages on the least squares as follows. Without the anomalous dispersion terms, the R (R_w) values were 0.0322 (0.0460), 0.0773 (0.0940), and 0.0639 (0.0770) for complexes **1′**, **3′**, and **5′**, respectively. In the cases of including the anomalous dispersion terms for all non-hydrogen atoms, the R (R_w) values of space group $P3_1$ were 0.0342 (0.0492), 0.0737 (0.0904), and 0.0595 (0.0713) for complexes **1′**, **3′**, and **5′**, respectively. The corresponding values for the inverted structure ($P3_2$) were 0.0295 (0.0418), 0.0801 (0.0980), and 0.0683 (0.0844). Thus, the absolute configuration was assigned to D-rich (D : L = 63 :37) for complex **1′**, L-rich (D : L = 32 : 68) for complex **3′**, and L-rich (D : L = 44 : 56%) for complex **5′**.

Full crystal data, H-atom coordinates, thermal parameters, $F_o - F_c$ tables, and remaining bond lengths and angles are given in the supplementary materials.[7]

Measurements. The absorbances were measured using a Hitachi 330 spectrophotometer, CD spectra with a JASCO J-500C spectropolarimeter, and IR spectra with a Shimadzu IR-435 spectrophotometer. X-Ray crystal analyses were carried out at the X-ray Diffraction Service of the Department of Chemistry.

Results and Discussion

Preparation and Characterization of Complexes. In the [Co(amino acidato-*N*,*O*)(tren)]X_2 type complex, there are two geometrical isomers, which are denoted as *cis*(*N*,*t*-*N*) and *trans*(*N*,*t*-*N*), concerning the mutual disposition between the NH_2 group of amino acidate and the tertiary amine of tren (Fig. 1). In the present leu, n-leu, and n-val systems, only one geometrical isomer (orange) was obtained. Complex **2** (L-leu) exhibits the first d–d band at 471 nm and two CD components, (+) at 510 and (−) at 455 nm, in the same region. The absorption maximum and CD pattern are the same as

Table 2. Equilibrium of the Ternary System, *trans*(*N*,*t*-*N*)-[Co(L-amino acidato)(tren)]-X_2–*trans*(*N*,*t*-*N*)-[Co(D-amino acidato)(tren)]X_2–H_2O, at 25 °C

Point no.	leu (X=I)			n-leu (X=ClO_4)			n-val (X=ClO_4)		
	Liquid phase (wt %)		Solid phase (%)	Liquid phase (wt %)		Solid phase (%)	Liquid phase (wt %)		Solid phase (%)
	S_L	S_D	L : D	S_L	S_D	L : D	S_L	S_D	L : D
1	1.26	1.26	63 : 37	1.27	1.27	68 : 32	1.06	1.06	44 : 56
2	1.42	1.06	68 : 32	1.34	1.14	69 : 31	0.98	1.12	39 : 61
3	1.49	0.92	72 : 28	1.48	0.89	76 : 24	0.80	1.22	31 : 69
4	1.56	0.78	76 : 24	1.67	0.51	85 : 15	0.60	1.30	26 : 74
5	1.73	0.51	83 : 17	1.81	0.23	93 : 7	0.49	1.42	20 : 80
6	1.80	0.42	88 : 12	1.87	0.10	97 : 3	0.29	1.55	11 : 89
7	1.89	0.28	91 : 9	1.96	0	100 : 0	0.18	1.63	7 : 93
8	1.92	0.17	96 : 4				0.04	1.68	2 : 98
9	2.03	0	100 : 0				0	1.70	0 : 100

Table 3. Crystal Data for Complexes **1′**, **3′**, and **5′**

	Complex **1′**	Complex **3′**	Complex **5′**
Formula	$C_{12}H_{30}O_2N_5CoI_2$	$C_{12}H_{30}O_{12}N_5CoCl_2$	$C_{11}H_{28}O_{10}N_5CoCl_2$
L : D	37 : 63	68 : 32	56 : 44
Fw	589.14	534.24	520.21
Space group	$P3_2$ (No. 145)	$P3_1$ (No. 144)	$P3_1$ (No. 144)
Cryst. size/mm	0.20×0.20×0.35	0.25×0.25×0.20	0.20×0.20×0.30
a/Å	9.193(2)	9.342(3)	9.308(1)
c/Å	20.798(3)	21.311(6)	20.952(2)
V/Å^3	1522.1(5)	1611.2(8)	1572.2(3)
Z	3	3	3
D_{calc}/g cm^{-1}	1.928	1.652	1.648
2θ range/deg	3—60	3—60	3—60
Temp/°C	23	23	23
h,*k*,*l*	±13,−13,+29	±13,+13,+30	+13,±13,−30
Variables	239	319	299
$I > 3\sigma(I)$	2711	1713	1443
R[a)]	0.027	0.071	0.055
R_w[b)]	0.037	0.078	0.062

a) $R = \Sigma||F_o| - |F_c||/\Sigma|F_o|$. b) $R_w = [(\Sigma w(|F_o| - |F_c|)^2/\Sigma w|F_o|^2)]^{1/2}$; $w = 1/\sigma^2(F_o)$.

those in *trans*(*N*,*t*-*N*)-[Co(L-val)(tren)]$^{2+}$ [orange isomer; L-val = L-valinate(1-)].[5,8] The norleucinato complexes, **3** (DL-n-leu) and **4** (L-n-leu), and the norvalinato complexes, **5** (DL-n-val) and **6** (D-n-val), also show similar absorption spectra to that of *trans*(*N*,*t*-*N*)-[Co(L-val)(tren)]$^{2+}$. Hence, complexes **1**—**6** are assigned to the *trans*(*N*,*t*-*N*) isomer.

Two isomers, orange and red, have so far been prepared

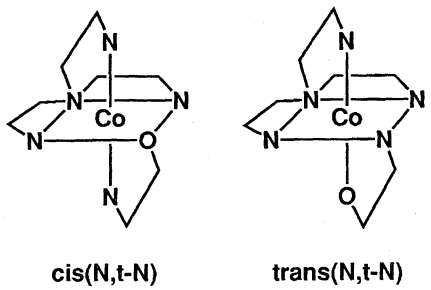

Fig. 1. Two geometrical isomers of [Co(amino acidato-*N*,*O*)-(tren)]$^{2+}$.

in [Co(glycinato)(tren)]$^{2+}$ [8] and [Co(L-alaninato)(tren)]$^{2+}$.[5] However, it is well known that the formation of the red *cis*(*N*,*t*-*N*) isomer decreases along with an increase in the bulkiness of a substituent on the amino carboxylate ring; only the orange isomer has been reported for each tren complex with L-valinate, L-serinate, L-phenylalaninate, and D-phenylglycinate.[5] The same phenomena were observed in the present leucinato, norleucinato, and norvalinato systems.

Solubility Phase Diagrams. Table 1 shows the binary solubilities of *trans*(*N*,*t*-*N*)-[Co(leu)(tren)]I_2 at 5—55 °C. Both solubility curves of the racemate and the enantiomer are smooth at 5—55 °C, which means the nonexistence of the polymorphism observed in the system of [$Co(CO_3)(en)_2$]-Br (en = ethane-1,2-diamine).[9] The racemate is more soluble than the enantiomer over the entire measured region. The solubility ratio (S_{DL}/S_L) is 1.23—1.26 in the range of 5—55 °C. These values are very close to $2^{1/3} = 1.26$, which is theoretically expected for a spontaneously resolvable MX_2 electrolyte.[10] The racemate and enantiomer are both anhydrate, and show the same infrared spectra. These facts ap-

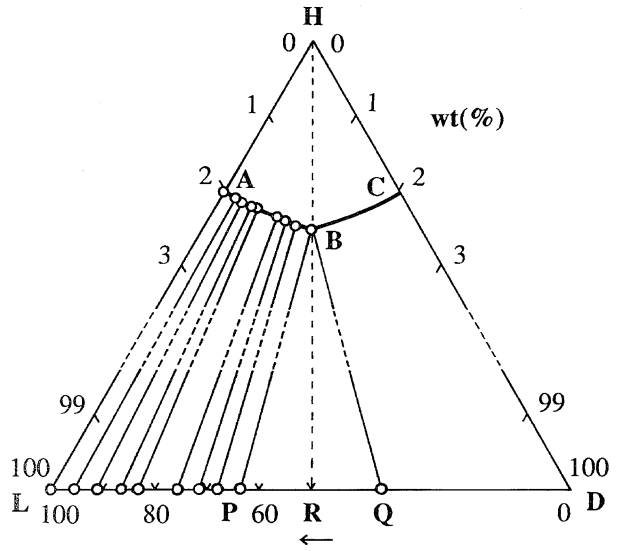

Fig. 2. Ternary solubility isotherm of the system, H_2O (**H**)–*trans*(*N*,*t*-*N*)-[Co(L-leu)(tren)]I_2 (**L**)–*trans*(*N*,*t*-*N*)-[Co(D-leu)(tren)]I_2 (**D**), at 25 °C. A single crystal at point **Q** is employed for X-ray analysis.

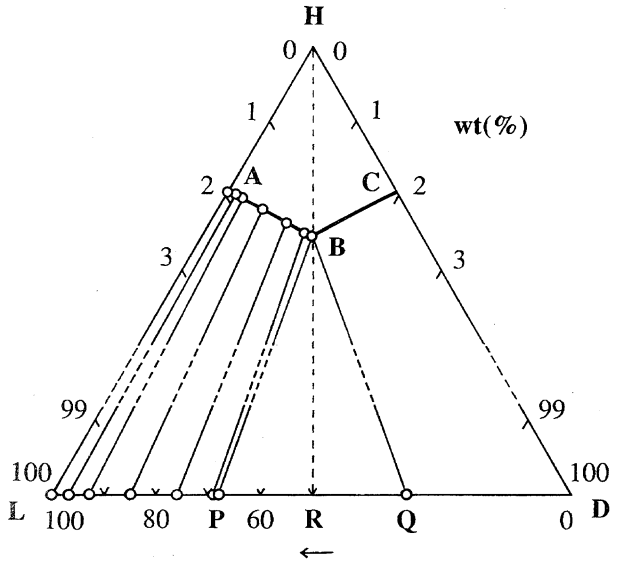

Fig. 3. Ternary solubility isotherm of the system, H_2O (**H**)–*trans*(*N*,*t*-*N*)-[Co(L-n-leu)(tren)][ClO_4]$_2$ (**L**)–*trans*(*N*,*t*-*N*)-[Co(D-n-leu)(tren)][ClO_4]$_2$ (**D**), at 25 °C. A single crystal at point **P** is employed for X-ray analysis.

parently mean that the racemic iodide forms a conglomerate at 5—55 °C.

To confirm the above expectation, we measured the ternary solubility isotherm of *trans*(*N*,*t*-*N*)-[Co(leu)(tren)]I_2 at 25 °C. In Fig. 2, the dotted line **HR** corresponds to the racemic composition, and lines **HL** and **HD** correspond to the compositions of the pure L- and D-complexes, respectively. Points **A** and **C** represent the equal solubilities of the pure enantiomers. The two branches of the solubility curve (**AB** and **BC**) separate the domain of unsaturated solutions. Point **B** denotes the eutectic where two solids (**P** and **Q**) coexist; there are no liquid lines equilibrated with the solid phases between

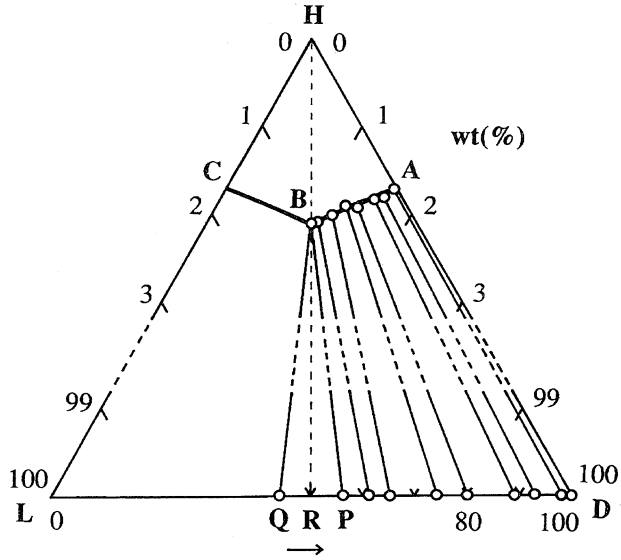

Fig. 4. Ternary solubility isotherm of the system, H_2O (**H**)–*trans*(*N*,*t*-*N*)-[Co(L-n-val)(tren)][ClO_4]$_2$ (**L**)–*trans*(*N*,*t*-*N*)-[Co(D-n-val)(tren)][ClO_4]$_2$ (**D**), at 25 °C. A single crystal at point **Q** is employed for X-ray analysis.

PQ. The isotherm denoting a racemic compound does not appear in the middle region (**BPQ**). These aspects seem to be typical for a conglomerate. However, it should be noted that the present system is definitively different from a normal conglomerate system concerning their tie lines. In a normal conglomerate all tie lines converge to the pure enantiomers, whereas the tie lines in this system diverge widely between two ranges of concentrations (**LP** and **QD**). For example, the saturated racemic solution is in equilibrium with two kinds of crystals of (D : L = 37 : 63) and (D : L = 63 : 37) at points **P** and **Q**, respectively. Similarly, each point on **AB** and **BC** is in equilibrium with a solid of 100—26% enantiomeric excess (ee). These facts lead to the conclusion that the present system forms a conglomerate and simultaneously a solid solution at 25 °C. The same ternary isotherm is expected over the entire region of 5—55 °C because the solubility ratio (S_{DL}/S_L) is constant at 5—55 °C (Table 1). This is the first example having both features of a conglomerate and a solid solution. We would like to call such a solid solution a conglomeratic solid solution.

In a normal conglomerate, where all liquid lines are tied with the pure enantiomers, optical resolution is easily achieved by crystallizing from a racemic solution and picking up one crystal, whereas the present *trans*(*N*,*t*-*N*)-[Co(leu)(tren)]I_2 is only partially resolved, because the equilibrated solid phase at **B** has only 26% ee. This circumstance is analogous in the purification of an optically impure enantiomer. Although the purification is easy in a normal conglomerate by recrystallization of the optically impure enantiomer, repeated recrystallizations would be necessary in the present system; moreover, we never reach the 100% ee point by fractional crystallization, because the optically impure saturated solution among **AB** (or **BC**) is not in equilibrium with the optically pure solid phase (**L** or **D**).

The situations in *trans*(*N*,*t*-*N*)-[Co(n-leu)(tren)][ClO_4]$_2$ and *trans*(*N*,*t*-*N*)-[Co(n-val)(tren)][ClO_4]$_2$ are very similar to that of *trans*(*N*,*t*-*N*)-[Co(leu)(tren)]I_2. Both of the solubility curves of the racemate and the enantiomer are smooth at 5—50 °C in *trans*(*N*,*t*-*N*)-[Co(n-leu)(tren)][ClO_4]$_2$. Both the racemate and enantiomer are anhydrate, and exhibit the same infrared spectra in each system. The solubility ratio (S_{DL}/S_L) in *trans*(*N*,*t*-*N*)-[Co(n-leu)(tren)][ClO_4]$_2$ is 1.19—1.33 in the 5—50 °C range (Table 1). The values are also close to $2^{1/3} = 1.26$. Figures 3 and 4 show the ternary isotherms of *trans*(*N*,*t*-*N*)-[Co(n-leu)(tren)][ClO_4]$_2$ and *trans*(*N*,*t*-*N*)-[Co-(n-val)(tren)][ClO_4]$_2$, respectively, at 25 °C. In these systems, each isotherm has two branches of the solubility curve and one eutectic; the tie lines diverge widely. The saturated racemic solution is in equilibrium with two kinds of crystals of (D : L = 32 : 68) and (D : L = 68 : 32) in *trans*(*N*,*t*-*N*)-[Co-(n-leu)(tren)][ClO_4]$_2$ and (D : L = 44 : 56) and (D : L = 56 : 44) in *trans*(*N*,*t*-*N*)-[Co(n-val)(tren)][ClO_4]$_2$. Thus, *trans*(*N*, *t*-*N*)-[Co(n-leu)(tren)][ClO_4]$_2$ has both properties of a conglomerate and a solid solution within the range of 5—50 °C and *trans*(*N*,*t*-*N*)-[Co(n-val)(tren)][ClO_4]$_2$ also forms a conglomeratic solid solution at 25 °C.

Molecular Structures. The single crystals in equilibrium with the racemic solution, which correspond to the solid of point (**P** or **Q**) in Figs. 2, 3, and 4, were grown at 25 °C. They are *trans*(*N*,*t*-*N*)-[Co(leu)(tren)]I_2 (**1′**), *trans*(*N*, *t*-*N*)-[Co(n-leu)(tren)][ClO_4]$_2$ (**3′**), and *trans*(*N*,*t*-*N*)-[Co-(n-val)(tren)][ClO_4]$_2$ (**5′**). The crystal data are summarized in Table 3. The numberings of non-hydrogen atoms are equal in **1′**, **3′**, and **5′**, except for the side chains of the amino acidates. The atomic coordinates of non-hydrogen atoms are given in Tables 4 (complex **1′**), 5 (**3′**), and 6 (**5′**). The selected bond distances and the bond angles of three complexes are given in Tables 7 and 8, respectively.

The ordered parts comprise the moieties, except for the asymmetric carbon (C(8)) and the side chain of the amino acidate in each complex. The structures of the ordered parts in complexes **1′**, **3′**, and **5′** are close to each other (Tables 7 and 8), and their bond length and angles are also similar to those of *trans*(*N*,*t*-*N*)-[Co(n-leu)(tren)]I_2 and *trans*(*N*,*t*-*N*)-[Co(met)(tren)]I_2.[3] On the other hand, the bond distances and angles concerning the amino acidates moieties are not normal, because there are disorders and simultaneously partial accidental overlaps concerning the asymmetric carbons (C(8)) and/or the side chains in the D- and L-amino acidates.

Figure 5 shows an ORTEP[11] drawing of the cation of *trans*(*N*,*t*-*N*)-[Co(leu)(tren)]I_2 (**1′**). Though two geometrical isomers are possible in the [Co(amino acidato-*N*,*O*)(tren)]$^{2+}$, complex **1′** adopts the *trans*(*N*,*t*-*N*) structure, as expected from the absorption spectrum. The figure clearly demonstrates the coexistence of D-leucinate and L-leucinate at one site of the crystal lattice, that is, a solid solution. The space group $P3_2$ means that the complex is spontaneously resolved. The D- and L-molecule ratio at each site was determined to be D : L = 63 : 37 in the same way as described elsewhere.[3] The value is the same as that obtained independently by solubility measurements. Thus, the crystal analytical result also confirms the fact that the saturated racemic solution is in equilibrium with two kinds of crystals of (D : L = 37 : 63) and (D : L = 63 : 37). These facts lead to the conclusion that the present system simultaneously forms a conglomerate and a solid solution.

Table 4. Positional and Isotropic-Equivalent Thermal Displacement Parameters (B(eq) in Å^2)[b] for *trans*(*N*,*t*-*N*)-[Co(leu)(tren)]I_2 (**1′**)

Atom	x	y	z	B(eq)
Co(1)	0.20351(8)	0.04136(7)	0	1.89(2)
O(1)	0.0846(5)	−0.0834(4)	0.0733(2)	2.4(1)
O(2)	−0.0747(5)	−0.0871(5)	0.1546(2)	3.2(1)
N(1)	0.2762(6)	−0.1155(6)	−0.0242(2)	2.8(2)
N(2)	0.4061(6)	0.1486(6)	0.0546(2)	2.8(1)
N(3)	0.3194(6)	0.1700(6)	−0.0757(2)	2.7(1)
N(4)	−0.0046(6)	−0.1047(5)	−0.0481(2)	2.6(1)
N(5)	0.1368(6)	0.2027(5)	0.0253(2)	2.5(1)
C(1)	0.378(1)	−0.1215(9)	0.0299(4)	4.0(3)
C(2)	0.4996(8)	0.054(1)	0.0494(4)	4.1(3)
C(3)	0.376(1)	−0.0585(9)	−0.0856(4)	4.1(2)
C(4)	0.4447(8)	0.1264(9)	−0.0981(3)	3.7(2)
C(5)	0.1204(9)	−0.2816(7)	−0.0331(3)	3.5(2)
C(6)	−0.0006(8)	−0.2559(7)	−0.0729(3)	3.4(2)
C(7)	0.0146(7)	−0.0185(7)	0.1076(3)	2.7(2)
C(8A)[a]	0.018(1)	0.143(1)	0.0812(4)	2.6(3)
C(8B)[a]	0.087(2)	0.167(2)	0.0956(6)	1.9(3)
C(9A)[a]	0.084(1)	0.284(1)	0.1334(5)	3.5(4)
C(9B)[a]	−0.035(2)	0.224(2)	0.1112(9)	3.4(6)
C(10)	0.058(1)	0.4288(8)	0.1123(3)	3.9(2)
C(11)	0.178(2)	0.560(2)	0.1617(5)	9.4(6)
C(12)	−0.105(1)	0.425(2)	0.1138(7)	8.0(6)
I(1)	0.90080(5)	0.25024(5)	−0.10003(2)	3.50(1)
I(2)	0.41963(5)	0.99088(6)	0.68701(3)	4.24(2)

a) The populations are 0.63 for C(8A) and C(9A), and 0.37 for C(8B) and C(9B). b) $B(\text{eq}) = (8\pi^2/3)\sum_{i=1}^{3}\sum_{j=1}^{3} U_{i,j} a_i^* a_j^* \boldsymbol{a}_i \cdot \boldsymbol{a}_j$.

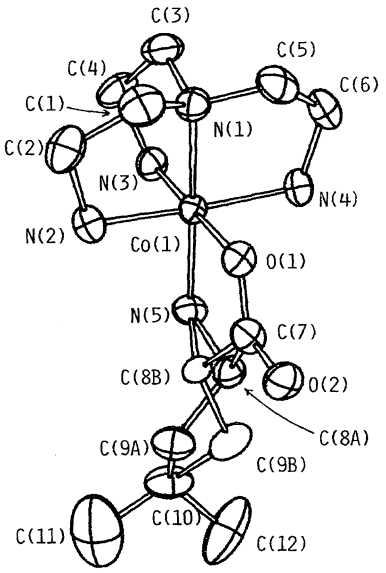

Fig. 5. An ORTEP drawing of *trans*(*N*,*t*-*N*)-[Co(leu)(tren)]I_2 (**1′**) with thermal ellipsoids drawn at the 50% probability level.

Table 5. Positional and Isotropic-Equivalent Thermal Displacement Parameters (B(eq) in Å^2)[b] for *trans*(*N*,*t*-*N*)-[Co(n-leu)(tren)][ClO_4]$_2$ (**3′**)

Atom	x	y	z	B(eq)
Co(1)	0.2038(2)	0.0434(2)	0	2.31(5)
O(1)	0.095(1)	−0.079(1)	−0.0739(4)	2.8(3)
O(2)	−0.051(1)	−0.081(1)	−0.1563(4)	3.8(4)
N(1)	0.273(1)	−0.110(1)	0.0258(5)	3.2(4)
N(2)	0.405(1)	0.148(1)	−0.0506(5)	3.8(5)
N(3)	0.307(1)	0.167(1)	0.0751(5)	3.3(4)
N(4)	0.001(1)	−0.093(1)	0.0452(5)	3.3(4)
N(5)	0.133(1)	0.199(1)	−0.0295(5)	3.7(5)
C(1)	0.378(2)	−0.116(2)	−0.0305(7)	4.6(7)
C(2)	0.487(2)	0.046(3)	−0.0486(8)	6.0(8)
C(3)	0.366(2)	−0.057(2)	0.0839(8)	5.0(7)
C(4)	0.430(2)	0.124(2)	0.0979(8)	4.9(7)
C(5)	0.117(2)	−0.277(2)	0.0305(8)	4.7(7)
C(6)	−0.004(2)	−0.249(2)	0.0696(6)	3.5(5)
C(7)	0.022(2)	−0.022(2)	−0.1069(6)	2.9(5)
C(8A)[a]	0.006(2)	0.121(2)	−0.0750(8)	2.4(6)
C(8B)[a]	0.082(4)	0.168(4)	−0.094(1)	2(1)
C(9A)[a]	0.021(3)	0.244(2)	−0.127(1)	3.7(8)
C(9B)[a]	−0.078(6)	0.189(6)	−0.099(2)	4(2)
C(10)	−0.004(2)	0.382(2)	−0.0975(8)	5.4(8)
C(11)	0.016(2)	0.515(2)	−0.1502(8)	6.6(9)
C(12)	0.184(3)	0.588(3)	−0.186(1)	9(1)
Cl(1)	0.8814(4)	0.2519(5)	0.0984(2)	4.4(2)
O(11)	0.847(4)	0.360(3)	0.092(2)	29(3)
O(12)	1.044(2)	0.294(3)	0.092(1)	12(1)
O(13)	0.815(2)	0.160(5)	0.0516(9)	24(2)
O(14)	0.788(3)	0.157(3)	0.1468(8)	15(1)
Cl(2)	0.4060(5)	0.9831(5)	−0.7019(2)	5.0(2)
O(21)	0.452(3)	0.954(3)	−0.7583(7)	14(1)
O(22)	0.242(1)	0.911(1)	−0.6834(8)	8.5(7)
O(23)	0.480(3)	1.137(2)	−0.693(2)	28(2)
C(24)	0.479(2)	0.920(4)	−0.668(1)	22(2)

a) The populations are 0.68 for C(8A) and C(9A), and 0.32 for C(8B) and C(9B). b) $B(\mathrm{eq}) = (8\pi^2/3)\sum_{i=1}^{3}\sum_{j=1}^{3} U_{ij} a_i^* a_j^* \boldsymbol{a}_i \cdot \boldsymbol{a}_j$.

Table 6. Positional and Isotropic-Equivalent Thermal Displacement Parameters (B(eq) in Å^2)[b] for *trans*(*N*,*t*-*N*)-[Co(n-val)(tren)][ClO_4]$_2$ (**5′**)

Atom	x	y	z	B(eq)
Co(1)	0.2207(1)	0.0514(1)	0	2.40(3)
O(1)	0.1124(7)	−0.0677(7)	−0.0749(3)	2.8(2)
O(2)	−0.034(1)	−0.0724(9)	−0.1593(3)	4.4(3)
N(1)	0.285(1)	−0.108(1)	0.0257(4)	3.8(3)
N(2)	0.427(1)	0.159(1)	−0.0482(4)	3.6(3)
N(3)	0.326(1)	0.171(1)	0.0783(4)	3.7(3)
N(4)	0.0116(9)	−0.0911(9)	0.0448(3)	3.0(3)
N(5)	0.156(1)	0.211(1)	−0.0299(3)	3.2(3)
C(1)	0.391(2)	−0.111(2)	−0.0292(6)	5.4(5)
C(2)	0.510(1)	0.053(2)	−0.0502(6)	5.4(5)
C(3)	0.382(2)	−0.052(2)	0.0871(6)	5.4(5)
C(4)	0.440(2)	0.126(2)	0.1018(6)	6.1(6)
C(5)	0.130(1)	−0.272(1)	0.0322(6)	4.4(4)
C(6)	0.010(1)	−0.240(1)	0.0699(5)	3.9(4)
C(7)	0.046(1)	−0.007(1)	−0.1110(4)	3.5(3)
C(8A)[a]	0.025(2)	0.139(2)	−0.080(1)	4.1(7)
C(8B)[a]	0.112(3)	0.183(3)	−0.098(1)	4.1(9)
C(9)	0.031(3)	0.254(2)	−0.1274(7)	10(1)
C(10)	0.037(2)	0.409(2)	−0.1052(7)	6.7(7)
C(11)	0.001(5)	0.503(4)	−0.148(1)	16(2)
Cl(1)	0.8985(3)	0.2729(3)	0.0939(1)	4.4(1)
O(11)	0.839(2)	0.351(2)	0.0542(8)	12.2(9)
O(12)	1.069(1)	0.339(2)	0.0957(7)	11.8(7)
O(13)	0.838(2)	0.120(2)	0.060(1)	14(1)
O(14)	0.807(2)	0.199(3)	0.1467(5)	14(1)
Cl(2)	0.3986(3)	0.9816(4)	−0.6964(2)	5.3(1)
O(21)	0.455(2)	0.950(2)	−0.7525(6)	11.2(8)
O(22)	0.227(1)	0.911(1)	−0.6890(7)	9.9(6)
O(23)	0.476(2)	1.144(2)	−0.690(2)	27(2)
C(24)	0.459(2)	0.922(2)	−0.6524(7)	14(1)

a) The populations are 0.56 for C(8A) and 0.44 for C(8B). b) $B(\mathrm{eq}) = (8\pi^2/3)\sum_{i=1}^{3}\sum_{j=1}^{3} U_{ij} a_i^* a_j^* \boldsymbol{a}_i \cdot \boldsymbol{a}_j$.

Figures 6 and 7 show ORTEP drawings of the cations of *trans*(*N*,*t*-*N*)-[Co(n-leu)(tren)][ClO_4]$_2$ (**3′**) and *trans*(*N*,*t*-*N*)-[Co(n-val)(tren)][ClO_4]$_2$ (**5′**), respectively. In Fig. 7, the C(9), C(10), and C(11) carbons have abnormal ellipsoids, because the side chains of the D- and L-amino acidates should be separately solved, but could only be solved as an accidental overlap. The structures in both systems are very similar to that of complex **1′**. The D- and L-amino acidates occupy the same site in the unit cell, which firmly indicates the existence of a solid solution. Each site of complexes **3′** and **5′** are L-rich (space group $P3_1$): the ratio of D : L is 37 : 63 for **3′** and 44 : 56% for **5′**, whose values are the same as those obtained independently by the solubility measurements. In conclusion, complexes **3′** and **5′** also simultaneously form a conglomerate and a solid solution, that is, a conglomeratic solid solution.

Crystal Structures. The three complexes are all isomorphous to each other in spite of having different amino acidates and counter ions. They are spontaneously partially

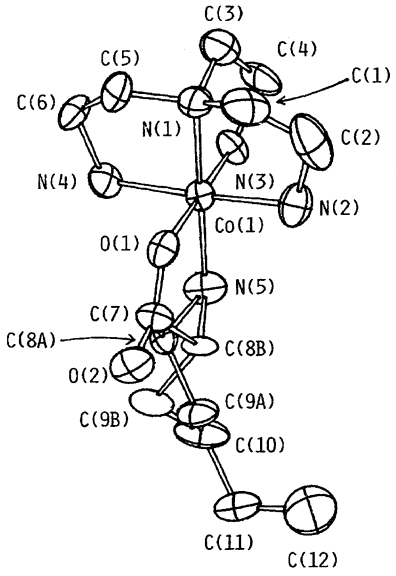

Fig. 6. An ORTEP drawing of *trans*(*N*,*t*-*N*)-[Co(n-leu)(tren)][ClO_4]$_2$ (**3′**) with thermal ellipsoids drawn at the 50% probability level.

Table 7. Selected Bond Distances (Å)

	Complex 1′	Complex 3′	Complex 5′
Co(1)–O(1)	1.893(3)	1.913(8)	1.894(5)
Co(1)–N(1)	1.935(7)	1.92(1)	1.93(1)
Co(1)–N(2)	1.973(5)	1.95(1)	1.948(8)
Co(1)–N(3)	1.936(4)	1.93(1)	1.950(8)
Co(1)–N(4)	1.974(4)	1.93(1)	1.962(7)
Co(1)–N(5)	1.940(6)	1.98(1)	1.96(1)
O(1)–C(7)	1.289(9)	1.26(2)	1.27(1)
O(2)–C(7)	1.229(7)	1.23(1)	1.22(1)
N(1)–C(1)	1.48(1)	1.57(2)	1.53(2)
N(1)–C(3)	1.504(9)	1.45(2)	1.51(2)
N(1)–C(5)	1.494(7)	1.51(1)	1.49(1)
N(2)–C(2)	1.50(1)	1.49(3)	1.53(2)
N(3)–C(4)	1.47(1)	1.47(3)	1.41(2)
N(4)–C(6)	1.500(9)	1.52(2)	1.48(1)
N(5)–C(8A)	1.50(1)	1.42(2)	1.49(2)
N(5)–C(8B)	1.52(1)	1.44(3)	1.46(2)
C(1)–C(2)	1.490(9)	1.39(3)	1.44(2)
C(3)–C(4)	1.51(1)	1.52(3)	1.49(2)
C(5)–C(6)	1.50(1)	1.52(3)	1.51(2)
C(7)–C(8A)	1.57(1)	1.57(3)	1.60(3)
C(7)–C(8B)	1.51(1)	1.60(4)	1.58(3)
C(8A)–C(9A)	1.56(1)	1.55(3)	—
C(8B)–C(9B)	1.49(3)	1.61(8)	—
C(8A)–C(9)	—	—	1.44(3)
C(8B)–C(9)	—	—	1.38(4)
C(9A)–C(10)	1.53(2)	1.55(3)	—
C(9B)–C(10)	1.63(2)	1.57(5)	—
C(9)–C(10)	—	—	1.49(3)
C(10)–C(11)	1.55(1)	1.62(3)	1.41(5)
C(10)–C(12)	1.48(2)	—	—
C(11)–C(12)	—	1.56(3)	—

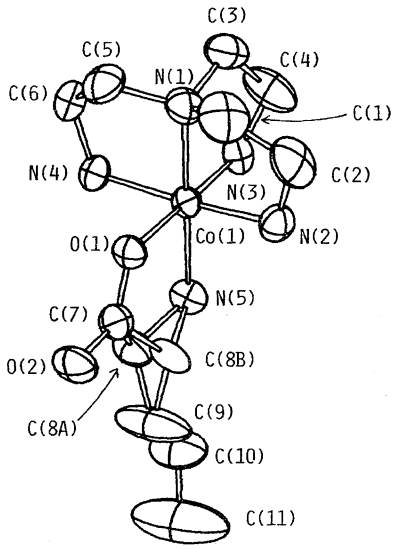

Fig. 7. An ORTEP drawing of *trans(N,t-N)*-[Co(n-val)-(tren)][ClO_4]$_2$ (**5′**) with thermal ellipsoids drawn at the 50% probability level.

resolved, and the single crystals used for the X-ray measurements are D-rich ($P3_2$) for **1′** and L-rich ($P3_1$) for **3′** and **5′**. Comparisons of the atomic coordinates for cobalt and iodide (or chlorine of perchlorate) in Tables 3, 4, and 5 clearly indicate the isomorphous relationship. The z value of iodide in complex **1′** has an opposite sign compared with that in complexes **3′** and **5′**.

Table 8. Selected Bond Angles (deg)

	Complex 1′	Complex 3′	Complex 5′
O(1)–Co(1)–N(5)	86.4(2)	84.4(4)	84.5(3)
N(1)–Co(1)–N(2)	86.0(2)	86.2(5)	86.3(4)
N(1)–Co(1)–N(3)	87.3(2)	87.4(5)	86.9(4)
N(1)–Co(1)–N(4)	86.5(2)	87.0(5)	86.0(4)
Co(1)–O(1)–C(7)	115.8(4)	116.5(9)	117.8(6)
Co(1)–N(1)–C(1)	106.8(5)	105(1)	104.8(8)
Co(1)–N(1)–C(3)	109.7(5)	111(1)	109.4(8)
Co(1)–N(1)–C(5)	106.4(5)	106(1)	107.2(8)
C(1)–N(1)–C(3)	112.0(6)	112(1)	112(1)
C(1)–N(1)–C(5)	110.8(5)	108(1)	110.7(9)
C(3)–N(1)–C(5)	110.9(5)	114(1)	112.6(8)
Co(1)–N(2)–C(2)	109.9(4)	109.6(9)	111.5(6)
Co(1)–N(3)–C(4)	111.0(4)	110(1)	110.9(8)
Co(1)–N(4)–C(6)	109.9(4)	111(1)	110.2(7)
Co(1)–N(5)–C(8A)	112.6(5)	110(1)	112(1)
Co(1)–N(5)–C(8B)	105.8(7)	111(2)	110(1)
N(1)–C(1)–C(2)	108.3(7)	108(2)	112(1)
N(2)–C(2)–C(1)	108.0(6)	112(1)	108(1)
N(1)–C(3)–C(4)	112.3(7)	113(2)	112(1)
N(3)–C(4)–C(3)	107.8(5)	108(1)	111(1)
N(1)–C(5)–C(6)	108.4(5)	106(1)	106.4(9)
N(4)–C(6)–C(5)	108.7(5)	108(1)	109.5(8)
O(1)–C(7)–O(2)	124.2(6)	126(1)	125(1)
O(1)–C(7)–C(8A)	117.9(5)	115(1)	115(1)
O(1)–C(7)–C(8B)	113.1(7)	114(2)	113(1)
O(2)–C(7)–C(8A)	117.0(7)	119(2)	117(1)
O(2)–C(7)–C(8B)	121.0(7)	117(2)	120(1)
N(5)–C(8A)–C(7)	106.2(8)	109(2)	104(2)
N(5)–C(8B)–C(7)	108.6(9)	106(2)	107(2)
N(5)–C(8A)–C(9A)	108.9(6)	111(1)	—
N(5)–C(8B)–C(9B)	109(1)	106(3)	—
N(5)–C(8A)–C(9)	—	—	115(1)
N(5)–C(8B)–C(9)	—	—	122(2)
C(7)–C(8A)–C(9A)	110.7(8)	108(1)	—
C(7)–C(8B)–C(9B)	112.2(9)	107(2)	—
C(7)–C(8A)–C(9)	—	—	112(2)
C(7)–C(8B)–C(9)	—	—	117(2)
C(8A)–C(9A)–C(10)	110.7(9)	110(2)	—
C(8B)–C(9B)–C(10)	111(1)	103(3)	—
C(8A)–C(9)–C(10)	—	—	118(1)
C(8B)–C(9)–C(10)	—	—	124(2)
C(9A)–C(10)–C(11)	97(1)	111(1)	—
C(9B)–C(10)–C(11)	132(1)	133(2)	—
C(9)–C(10)–C(11)	—	—	120(2)
C(9A)–C(10)–C(12)	124.9(8)	—	—
C(9B)–C(10)–C(12)	92(1)	—	—
C(10)–C(11)–C(12)	—	112(2)	—
C(11)–C(10)–C(12)	109(1)	—	—

There exists a head-to-tail contact between the carbonyl group of amino acidate and two amino groups of tren, as shown in Fig. 8. It should be noted that these double hydrogen bonds exist along the c-axis and form spiral chains.

The distances are as follows: O(2)---N(3) (or N(4)) $(y-x, -x, 1/3+z) = 2.857(6)$ [or 2.888(6)] for complex **1′**, O(2)---N(3) (or N(4)) $(y-x, -x, -1/3+z) = 2.85(1)$ [or

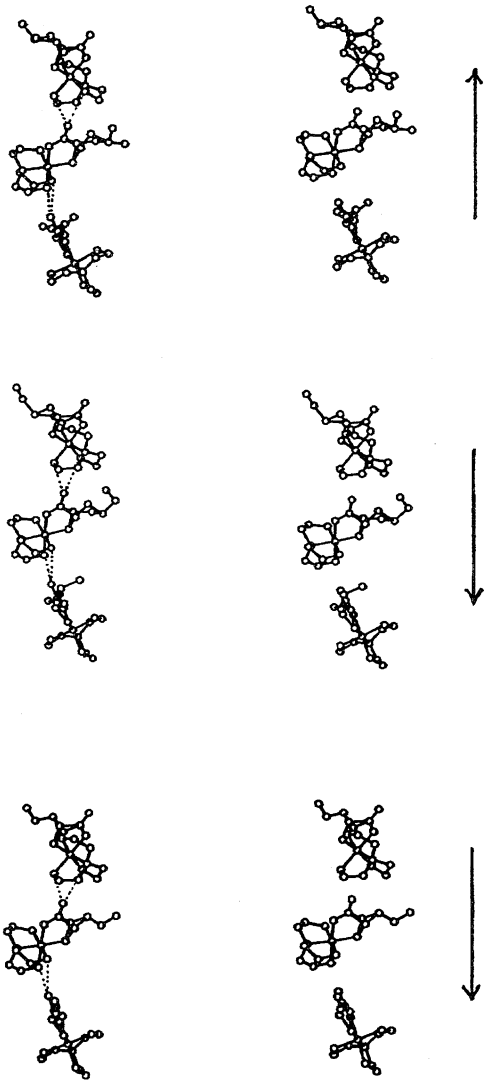

Fig. 8. Stereoviews of the hydrogen bond sequence in complexes **1′** (upper), **3′** (middle), and **5′** (lower). The broken lines show the hydrogen bonds between N(3) (or N(4)) and O(2). The arrows indicate their *c*-axis.

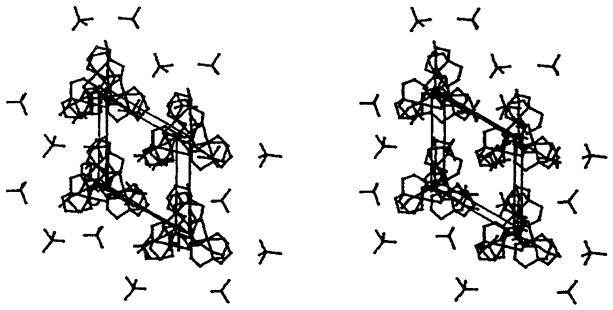

Fig. 9. Stereoview of the crystal packing of complexes **5′** viewed along *c*-axis.

2.98(1)] for complex **3′**, and O(2)- - -N(3) (or N(4)) ($y-x$, $-x$, $-1/3+z$) = 2.86(1) [or 2.90(1)] for complex **5′**. The chirality of the spiral in complex **1′** is opposite to those in complexes **3′** and **5′**. The spiral pitch, comprising three complex cations, corresponds to the length of the *c*-axis. Figure 9 shows a stereoview of the crystal packing of complex **5′**. The spiral columns along the *c*-axis are easily understandable. The distance between the spiral columns is equal to the length of the *a*-axis. This hydrogen-bonding interaction is responsible for the conglomeratic property in the present three complexes. In *trans*(*N*,*t*-*N*)-[Co(n-leu)(tren)]I_2 and *trans*(*N*,*t*-*N*)-[Co(met)(tren)]I_2, although a double head-to-head contact has been found, the hydrogen bonding interaction is limited between two cations and does not form a spiral sequence.[3] Therefore, complexes *trans*(*N*,*t*-*N*)-[Co(n-leu)(tren)]I_2 and *trans*(*N*,*t*-*N*)-[Co(met)(tren)]I_2 form a different solid solution from the present conglomeratic solid solution.

Conclusion Remarks. The present three complexes (*trans*(*N*,*t*-*N*)-[Co(leu)(tren)]I_2, *trans*(*N*,*t*-*N*)-[Co(n-leu)(tren)][ClO_4]$_2$, and *trans*(*N*,*t*-*N*)-[Co(n-val)(tren)][ClO_4]$_2$) all form unprecedented conglomeratic solid solutions which have both features of a conglomerate and a solid solution. They have been firmly characterized by solubility isotherms and X-ray crystal structure analyses. Our results suggest that a conversional classification in which crystalline racemates belong to one of three different classes (a racemic compound, a conglomerate, or a solid solution) is not adequate,[1] and that more diverse intermediate cases are expected to exist in the complexes of *trans*(*N*,*t*-*N*)-[Co(amino acidato-*N*,*O*)(tren)]X_2.

This work was partly supported by a Grant-in-Aid for Scientific Research No. 07640750 for K. Y. from the Ministry of Education, Science, Sports and Culture.

References

1) J. Jacques, A. Collet, and S. H. Wilen, "Enantiomers, Racemates, and Resolutions," Wiley, New York (1981).

2) A. Fuyuhiro, K. Hibino, and K. Yamanari, *Chem. Lett.*, **1991**, 1041.

3) K. Yamanari and A. Fuyuhiro, *Bull. Chem. Soc. Jpn.*, **68**, 2543 (1995).

4) K. Yamanari and A. Fuyuhiro, *Chem. Lett.*, **1991**, 1551.

5) K. Akamatsu, T. Komorita, and Y. Shimura, *Bull. Chem. Soc. Jpn.*, **54**, 3000 (1981).

6) "TEXRAY Structure Analysis Package," Molecular Structure Corporation, 1985.

7) They are deposited as Document No. 69023 at the Office of the Editor of Bull. Chem. Soc. Jpn.

8) Y. Mitsui, J. Watanabe, Y. Harada, T. Sakamaki, Y. Iitaka, Y. Kushi, and E. Kimura, *J. Chem. Soc., Dalton Trans.*, **1976**, 2095.

9) K. Yamanari and A. Fuyuhiro, *J. Chem. Soc., Dalton Trans.*, **1991**, 2903.

10) K. Yamanarai, J. Hidaka, and Y. Shimura, *Bull. Chem. Soc. Jpn.*, **46**, 3724 (1973).

11) C. K. Johnson, "ORTEP II. Report ORNL-5138," Oak Ridge National Laboratory, Oak Ridge, TN (1976).